# Spatio-temporal analysis of compound hydro-hazard extremes across the UK

Annie Visser-Quinn [a,*], Lindsay Beevers [a], Lila Collet [b], Guiseppe Formetta [c], Katie Smith [c], Niko Wanders [d], Stephan Thober [e], Ming Pan [f], Rohini Kumar [e]

[a] *Institute for Infrastructure and Environment, School of Energy, Geoscience, Infrastructure and Society, Heriot-Watt University, Edinburgh, UK*
[b] *Irstea, 1 rue Pierre Gilles de Gennes, 92 160 Antony, France*
[c] *Centre for Ecology & Hydrology, Wallingford, Oxfordshire OX10 8BB, UK*
[d] *Department of Physical Geography, Utrecht University, Princetonlaan 8A, 3508CB Utrecht, the Netherlands*
[e] *Helmholtz Centre for Environmental Research - UFZ, Leipzig, Germany*
[f] *Department of Civil and Environmental Engineering, Princeton University, Princeton, NJ, USA*

## ABSTRACT

There exists an increasing need to understand the impact of climate change on the hydrological extremes of flood and drought, collectively referred to as 'hydro-hazards'. At present, current methodology are limited in their scope, particularly with respect to inadequate representation of the uncertainty in the hydroclimatological modelling chain.

This paper proposes spatially consistent comprehensive impact and uncertainty methodological framework for the identification of compound hydro-hazard hotspots – hotspots of change where concurrent increase in mean annual flood and drought events is projected. We apply a quasi-ergodic analysis of variance (QE-ANOVA) framework, to detail both the magnitude and the sources of uncertainty in the modelling chain for the mean projected mean change signal whilst accounting for non-stationarity. The framework is designed for application across a wide geographical range and is thus readily transferable. We illustrate the ability of the framework through application to 239 UK catchments based on hydroclimatological projections from the EDgE project (5 CMI5-GCMs and 3 HMs, forced under RCP8.5).

The results indicate that half of the projected hotspots are temporally concurrent or temporally successive within the year, exacerbating potential impacts on society. The north-east of Scotland and south-west of the UK were identified as spatio-temporally compound hotspot regions and are of particular concern. This intensification of the hydrologic dynamic (timing and seasonality of hydro-hazards) over a limited time frame represents a major challenge for future water management.

Hydrological models were identified as the largest source of variability, in some instances exceeding 80% of the total variance. Critically, clear spatial variability in the sources of modelling uncertainty was also observed; highlighting the need to apply a spatially consistent methodology, such as that presented. This application raises important questions regarding the spatial variability of hydroclimatological modelling uncertainty. In terms of water management planning, such findings allow for more focussed studies with a view to improving the projections which inform the adaptation process.

## 1. Introduction

Hydrological hazards are defined as extreme events associated with the occurrence, movement and distribution of water, specifically floods and droughts (National Research Council, 1999; Collet et al., 2018). Flood hazards are the result of excess water from one or multiple sources (e.g. coastal, fluvial, or surface/sub surface water), while drought hazards arise from a deficit of river flow or precipitation over a prolonged period. Henceforward, we collectively term flood and drought as 'hydro-hazards'.

Climate change is significantly altering hydrological dynamics, with a general tendency to amplify hydrological extremes (Fischer and Knutti, 2016; Schleussner et al., 2017; Marx et al., 2018; Samaniego et al., 2018; Thober et al., 2018; Vousdoukas et al., 2018) and thus increase the influence on exposed populations and economic assets. At present, these changes are not widely understood due to the complex interactions between climate & hydrological systems and their regional

---

**Table 1**
Classification of compound hydro-hazards in this study.

| Name | Definition |
|---|---|
| Compound hydro-hazard hotspot | Concurrent increase in hydro-hazard (metrics) above a defined threshold. No additional spatial or temporal aspect. |
| Spatially compound hydro-hazard hotspot(s) | Compound hydro-hazard hotspot *AND* spatially compound at the intra-catchment level (nested sub-catchments, e.g. headwaters) and/or inter-catchment level (i.e. adjacent hotspots). |
| Temporally compound hydro-hazard hotspot | Compound hydro-hazard hotspot *AND* temporally compound (i.e. seasonal hotspots), where inter-annual drought and flood events are likely to occur concurrently within a given season (e.g. flood and drought occurring in JJA) or in consecutive seasons (e.g. flood occurring in JJA, followed by drought in SON). |
| Spatio-temporally compound hydro-hazard hotspot regions | Regions where the compound hydro-hazard hotspots are both spatially and temporally compound. |

variations (e.g. Manfreda and Caylor, 2013; Devkota and Gyawali, 2015; Collet et al., 2018; Li et al., 2018). During the period 2000–2015, hydro-hazards directly affected almost one million people in the UK, at a total estimated cost of 36 billion GBP (Guha-Sapir et al., 2018). Accordingly, it is necessary to consider changes in hydrological dynamics and flow regimes at present and in the future.

Typically, hydro-hazards are considered independently in water management planning. In the UK, hydrological impact assessments of climate change have, largely, focussed exclusively on either high flows (Prudhomme et al., 2012; Kay et al., 2014a, 2014b; Sayers et al., 2016; Collet et al., 2017) or low flows (Christierson et al., 2012; Watts et al., 2015; Marx et al., 2018). Further, inconsistencies in methodology lead to conflicting reports of the hydrological impact of climate change in the UK. Examples include disparities at the spatial scale (Kay et al., 2014a, 2014b; Watts et al., 2015) or in the climate projections used (Collet et al., 2017; Marx et al., 2018; Thober et al., 2018). Overall, Collet et al. (2018), Marx et al. (2018) and Thober et al. (2018) suggest a general increase in hydrological extremes across the UK, especially in the south west of England, west of Wales and north-east of Scotland, whilst, Kay et al. (2014a and b) report the greatest change in high flows in the north-west of Scotland. To ensure a holistic understanding, there is a clear need to consider changing hydro-hazards concurrently, i.e. both ends of the hydrological cycle must be explored at the same time.

In addition to the increased severity and frequency of hydro-hazards under climate change, compound events may exacerbate the impact on society (Hao et al., 2018). In IPCC (2012), the Intergovernmental Panel on Climate Change (IPCC) define compound events as *(1) two or more extreme events occurring simultaneously or successively, (2) combinations of extreme events with underlying conditions that amplify the impact of the events, or (3) combinations of events that are not extremes in themselves but lead to an extreme event or impact when combined* (i.e. clustered multiple events). These compound events need not occur simultaneously, they may also be the result of successive contrasting extremes, such as drought and flood (IPCC, 2012). Examples include the successive drought and flood events of 2010–2012 and 2015–2016 in the UK (Parry et al., 2013) and Tasmania, Australia respectively (CSIRO, 2018), and the ongoing concurrent drought-flood in Queensland, Australia (Butterworth and Margolis, 2019). In order to build resilience for climate change adaptation, there is a need to further characterise the spatial and temporal clustering of compound extremes (Hao et al., 2018).

The flow projections used in climate change impact assessment studies are the outputs of a long and complex modelling chain: General Circulation Models (GCMs) are forced by emissions scenarios, the outputs of which are downscaled to the regional scale, where hydrological models (HMs) propagate the climate signal, producing hydrological outputs such as discharge, soil moisture and groundwater recharge. With each of these (modelling) steps, uncertainty (in the model structure, input and parameters) cascades, propagating (or constraining) the uncertainty through the modelling chain (Warmink et al., 2010; Smith et al., 2018). Differences in HM structure have been identified as a source of uncertainty that should not be neglected (Dankers et al., 2014; Donnelly et al.,

2017; Gosling et al., 2017). One approach to the portioning of uncertainty is the quasi-ergodic analysis of variance (QE-ANOVA) (Hawkins and Sutton, 2009; Hingray and Saïd, 2014; Vidal et al., 2016; Hingray et al., 2019), which through a quasi-ergodic assumption, is able to account for the non-stationarity of climate change.

This paper proposes a spatially consistent comprehensive impact and uncertainty methodological framework for the identification of compound hydro-hazard hotspots. In the context of the framework, four classes of compound hydro-hazard hotspots are defined (Table 1): compound, spatially compound, temporally compound and spatio-temporally compound. The framework sees the determination of the concurrent change in the mean annual hydro-hazard from the baseline to future. In this way, it is possible to identify hotspots of change where hydro-hazards intensify or emerge under a changing climate. We term these compound hydro-hazard hotspots (i.e. intra-annual "successive contrasting extremes", as per the IPCC definition previously). Consideration of the spatial and temporal clustering of hotspots determines whether these compound hydro-hazard hotspots are spatial and/or temporally clustered.

The framework is presented through application to 239 catchments across the UK using transient climate projections (1970–2099). Compound hydro-hazard hotspots are identified for the far-future, 2071–2099. The objectives of the framework are two-fold:

(1) To identify, classify (Table 1) and analyse compound hydro-hazard hotspots;
(2) To quantify and characterise the sources of uncertainty in the hydroclimatological modelling chain using a QE-ANOVA framework; with a view to understanding the total and fractional uncertainty associated with the hydro-hazard projections.

The novelty of this impact and uncertainty framework lies in the classification of the compound hydro-hazard extremes in a spatial and temporal context. The proposed framework allows for the explicit quantification of the uncertainty in the projected hydro-hazard hotspots, thereby facilitating a greater understanding of future water (in) security.

## 2. Data

In this study, the methodological framework was applied across the United Kingdom of Great Britain and Northern Ireland (UK). Daily flow projections were drawn from the EDgE project (End-to-end Demonstrator for improved Decision-making in the water sector in Europe; C3S, 2018), a two-year proof-of-concept funded by the Copernicus Climate Change Service. The EDgE project combined climate data and state-of-the-art hydrological modelling to estimate river flows, as well as a range of Sectoral Climate Impact Indicators, across the European domain (http://edge.climate.copernicus.eu). For additional information see Wanders et al. (2018).

### 2.1. Models

The EDgE project utilised a multi-model ensemble of GCMs and HMs to capture uncertainty in the modelling process. Known to provide good coverage of the CMIP5 range of uncertainty (McSweeney and Jones, 2016), the EDgE project utilised the ISI-MIP (Inter-Sectoral Impact Model Intercomparison Project; https://www.isimip.org) subset of five GCMs (Warszawski et al., 2014): *HadGEM2-ES, GFDL-ESM2, IPSL-CM5A-LR, MIROC-ESM-CHEM* and *NorESM1-M*. Details on the processing of the GCM projections can be found in Marx et al. (2018). The four HMs used in EDgE are mHM (Samaniego et al., 2010; Kumar et al., 2013), Noah-MP (Niu et al., 2011; Yang et al., 2011), VIC (Liang et al., 1996; Cherkauer et al., 2003), and PCR-GLOBWB2 (Sutanudjaja et al., 2018). The HMs simulate surface and subsurface runoff as well as other land states/fluxes (e.g. evapotranspiration and soil moisture). The models Noah-MP and VIC are classified as land-surface models, capturing land-atmosphere interactions, whilst mHM and PCR-GLOBWB2 are focussed on water balance components only.

For consistency and efficiency, a single river routing model mRM (Samaniego et al., 2010) was used to derive river flows based on gridded runoff calculations output by the HMs. The mRM model is based on the Muskingum algorithm and is able to estimate streamflow at various spatial resolutions without recalibration of parameters (Thober et al., 2018, 2019). The HMs were validated for high, medium and low flows across a diverse range of European catchments (Marx et al., 2018; Samaniego et al., 2018; Thober et al., 2018).

In the validation of the flow projections, outputs from PCRGLOB-WB2 were, often, uniform in nature, failing to capture the processes leading to high/low flows. The lack of clearly defined peak flows meant that the necessary event extraction was not possible (see Section 3.1.). Consequently, flow projections from PCRGLOB-WB2 were not considered in this study. The validation of the EDgE flow projections is further considered in Appendix A.1.

### 2.2. Emissions scenarios

The EDgE project considered simulations of transient historical (1971–2000) and future (2011–2099) climate under both RCP2.6 and RCP8.5, the lowest and highest representative concentration pathways (RCPs), respectively. The focus of this study is RCP8.5, which formed part of the core experiments under CMIP5 (Taylor et al., 2011). RCP8.5 represents a high-emission trajectory, the result of no explicit implementation of climate policy, leading to a global mean temperature increase of 2.6–4.8 °C by the end of the century (Riahi et al., 2011).

### 2.3. Catchments

The catchment selection process is detailed in Appendix A.2. In this study, a total of 239 gauges were considered across 142 parent and 97 child (sub) catchments. The total catchment area covers 47,785 km$^2$ of the UK; their spatial distribution is illustrated in Fig. 1. Fig. 1 also highlights a north-south division in population distribution, ranging from 100,000 in the North of Scotland, to over 3,000,000 in the East Midlands and South-east England. Thirty-six percent of the population of the UK (based on an estimate of 66 million in November 2018; ONS, 2018) are located within the modelled catchment areas. From the perspective of the number of people exposed, a greater proportion of the population is likely to be impacted due to incurred losses (e.g. water supply, infrastructure, crop yield, etc.).

### 3. Methods

This paper proposes a spatially consistent comprehensive impact and uncertainty methodological framework for the identification of compound hydro-hazard hotspots. An overview of the three stages of the proposed framework is presented in Fig. 2. In stage 1, hydro-hazard
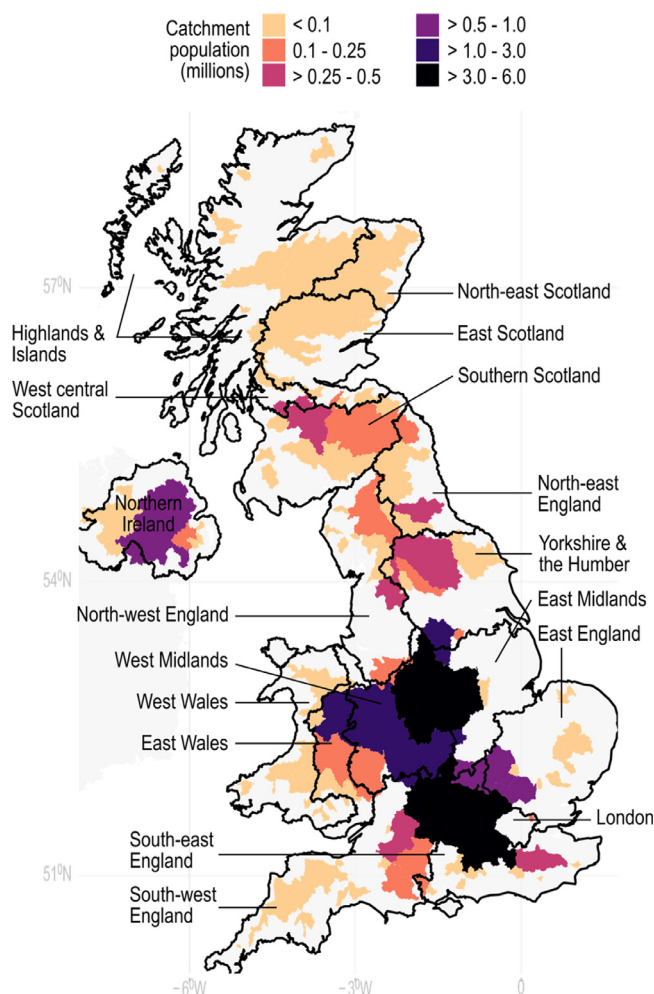


**Fig. 1.** Spatial distribution and population (in millions) of the 142 parent catchments considered in this study. Population data is based on gridded 1 km data from Reis et al. (2017). For reference, administrative regions are labelled and outlined in black.

events are identified and event metrics extracted per modelling chain, per catchment. From this, annual summary metrics and mean annual metrics are determined. The second stage sees the determination of the change signal, the mean change (across the modelling chains) in the mean annual metrics from the baseline (1971–2000) to the far-future (2071–2099) per catchment; compound hydro-hazard hotspots are subsequently classified (Table 1). In stage 3, the uncertainty is characterised following the QE-ANOVA approach: a noise-free-signal is determined per modelling chain, per catchment, followed by application of the ANOVA at the catchment level. The application of the framework is discussed with reference to the 239 catchments across the UK described in the previous section.

### 3.1. Stage 1. Identification of hydro-hazards

Stage 1 begins with event extraction (Fig. 2, 1.1). Following Collet et al. (2018), catchment streamflow thresholds for the extraction of flood and drought events were defined on the baseline (historic simulations 1971–2000) for a mean of three independent events per annum across the 15 hydroclimatological modelling chains (5 GCMs and 3 HMs). For each catchment and modelling chain, flood events were extracted from the peak over threshold (POT) time-series, following Bayliss and Jones (1993), where a flood event is defined as a period when daily flow is continuously above the defined threshold (for an av-
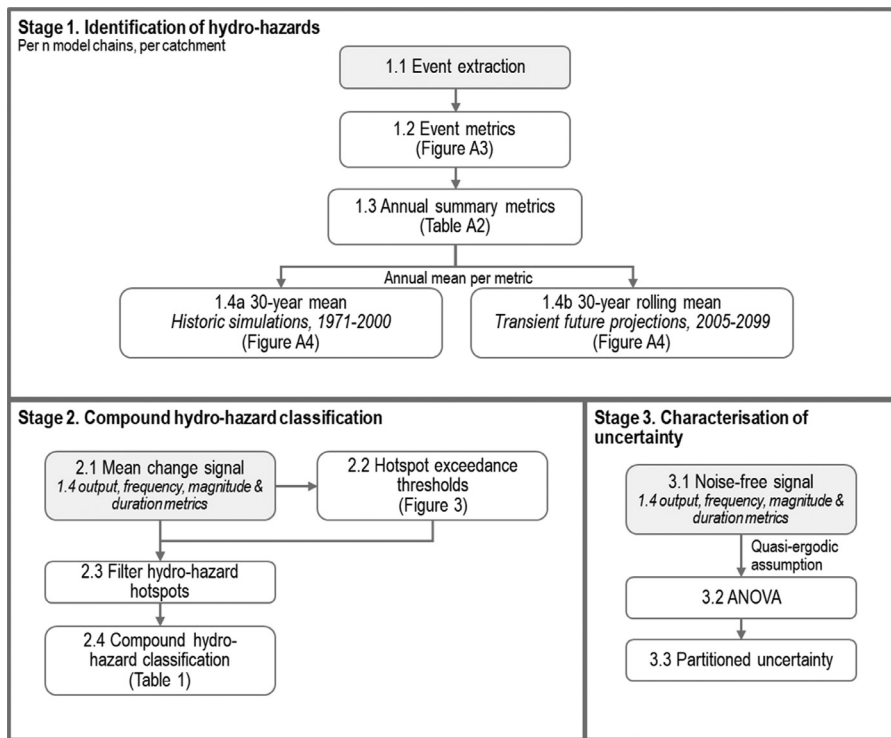
Fig. 2. The proposed impact and uncertainty methodological framework for the identification of compound hydro-hazard hotspots. Each step is numbered, and the start points for each stage of the framework shaded.

erage of three POT per annum). Drought equivalent characteristics were determined using the R package `lfstat` (version 0.9.4; Koffler et al., 2016). In `lfstat`, a drought event occurs when daily flow falls below a given threshold; here, a varying Q90 threshold (defined as the flow equally or exceeded 90% of the time) was specified per Julian day (i.e. 365 thresholds). Independent drought events were identified by applying the inter-event time and volume criterion method (Gustard and Demuth, 2009; Koffler et al., 2016); events were pooled where the inter-event time is less than 5 days and the drought to inter-event volume ratio fell below 0.1.

Three event metrics (1.2), describing the duration, timing (day of year) and magnitude (peak flow and flow deficit volume below threshold for flood and drought respectively) were determined for each independent event (for details, see Fig. A3). From these event metrics, annual summary metrics (1.3) were subsequently determined; a count of the number of independent events per year (frequency) was also made. The annual mean, per metric, was then determined (1.4); for the historic simulation (1971–2000) this represents the 30-year mean, whilst for the transient future projections (2005–2099) a 30-year rolling mean was determined (for example, 2011–2040, 2012–2041 and so on). The mean annual metrics represent the data input to stages 2 and 3 (Fig. 2).

### 3.2. Stage 2. Compound hydro-hazard classification

Stage 2 utilises the outputs from stage 1, 1.4. For each catchment, the mean change signal (2.1) from the baseline (1971–2000) to far-future (2071–2099) was determined for the frequency, magnitude and duration metrics per catchment, per modelling chain. The mean change signal across the 15 modelling chains was subsequently determined per catchment.

In the framework, a compound hydro-hazard is the concurrent increase in the mean annual frequency, magnitude and duration of flood and drought events (total six metrics). A compound hydro-hazard hotspot represents a concurrent increase in these six metrics above a defined threshold, $T$ (Table 1 and Fig. 3, region IV). After Collet et al. (2018), a sensitivity analysis was applied to determine
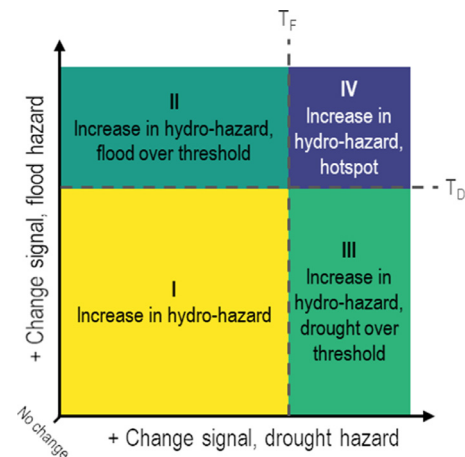


Fig. 3. Matrix describing the four regions of increase in the annual compound hydro-hazard. The change is concurrent for the mean annual frequency, magnitude and duration metrics for flood and drought. $T_F$ and $T_D$ represent the flood and drought thresholds respectively.

**Table 2**
Mean change signal thresholds for compound hydro-hazard hotspot identification.

| Mean annual metric | Drought | Flood |
|---|---|---|
| Frequency (events per year) | ≥1 | ≥1 |
| Magnitude (% per year) | ≥50 | ≥5 |
| Duration (days per year) | ≥10 | ≥3 |

exceedance thresholds above which 20% of the catchments lie (2.2; Table 2).

The hydro-hazard hotspots (2.3) were further classified (2.4) into different types of compound hydro-hazard as per Table 1. The temporal aspect is represented by the mean annual time of year and the degree of seasonality in the far-future (2071–2099; 1.4b). Seasonality is defined
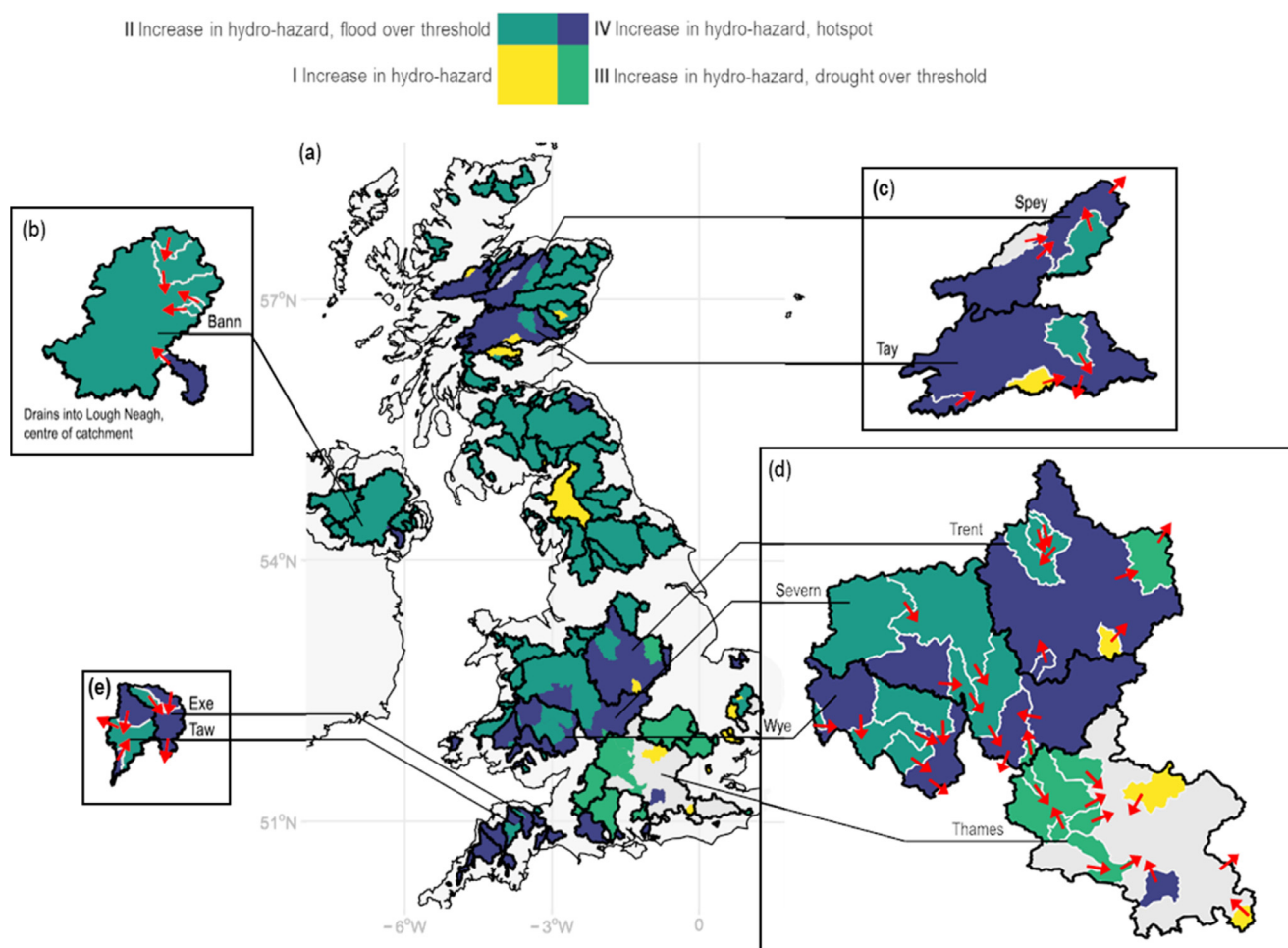
**Fig. 4.** Spatial distribution of (a) all catchments where there is an increase in the compound hydro-hazard in the far-future. Inset (b) to (e): 2.5× magnification of nested catchments where hotspots are projected. Parent catchments are outlined in black, child catchments (nested sub-catchments) are outlined in grey; arrows indicate the direction of flow from headwaters to outflow.

as the concentration of events around the 30-year mean Julian Day (determined using circular statistics following the approach of Bayliss and Jones, 1993 and Institute of Hydrology, 1999; for example calculations see supplement in Formetta et al., 2018). A value of zero indicates a lack of seasonality, where events are widely dispersed throughout the year, whilst a value greater than 0.6 indicates that events are concentrated at a particular time of year (Formetta et al., 2018), i.e. seasonally occurring events.

### 3.3. Stage 3. Characterisation of uncertainty

The spatial variability of the hydroclimatological modelling uncertainty associated with the annual mean frequency, magnitude and duration metrics was determined through the application of a QE-ANOVA approach per catchment. Thus, the total uncertainty may be partitioned in terms of the relative contribution of each source of uncertainty. This method is based on the quasi-ergodic assumption for transient climate simulations (Hingray and Saïd, 2014), where, for a sufficiently long time period, it is assumed that all possible states are captured, thereby reducing the extrapolation out with the sample space. The QE-ANOVA approach accounts for both modelling uncertainty and internal variability. The internal variability represents the variation of climate on both a large- and local-scale, representing natural fluctuations of climate and variation in local meteorology respectively; this variation may be observed through multiple evolutions of a given GCM and downscaling model. In this study, the residuals capture both the internal variability

and statistical downscaling uncertainty (as only one method is applied – based on geostatistical, External Drift Kriging; see Marx et al., 2018). It should be noted that the quasi-ergodic assumption is only applicable for sufficiently large sample sizes, the ratio of the time-series length to the size of the sliding window. Here, the sample size of 4.17 (1971–2099, 125/30 yr) is deemed suitable, being comparable with previous studies such as Vidal et al. (2016), sample size 4.25 (1980–2065, 85/20 yr).

The first stage of the QE-ANOVA approach sees the determination of the noise-free signal (NFS; 3.1) per catchment, per modelling chain. For each metric, linear trendlines were fitted to both the baseline simulations and transient projections. After Vidal et al. (2016), a linear trend model was selected to prevent overfitting of inter-annual fluctuations; the baseline linear model was also fixed due to a relatively short baseline period. The NFS per modelling chain, $m$, at time $t$ represents the change in the trend model output $y$ relative to the average of the baseline trend model, $Y_0$. Following Hingray and Saïd (2014), the NFS is defined as:

$$NFS(m,t) = y(m,t) - Y_o \tag{1}$$

for the absolute change in frequency and duration, and:

$$NFS(m,t) = \frac{y(m,t)}{Y_o} - 1 \tag{2}$$

for the relative change in magnitude.

Following a classical two-way ANOVA framework (3.2), without interaction, the NFS was partitioned into the variance associated with the GCM & HM, and residuals (for a three-way ANOVA see Vidal et al., 2016). For further details see Hingray and Saïd (2014). The sum of these
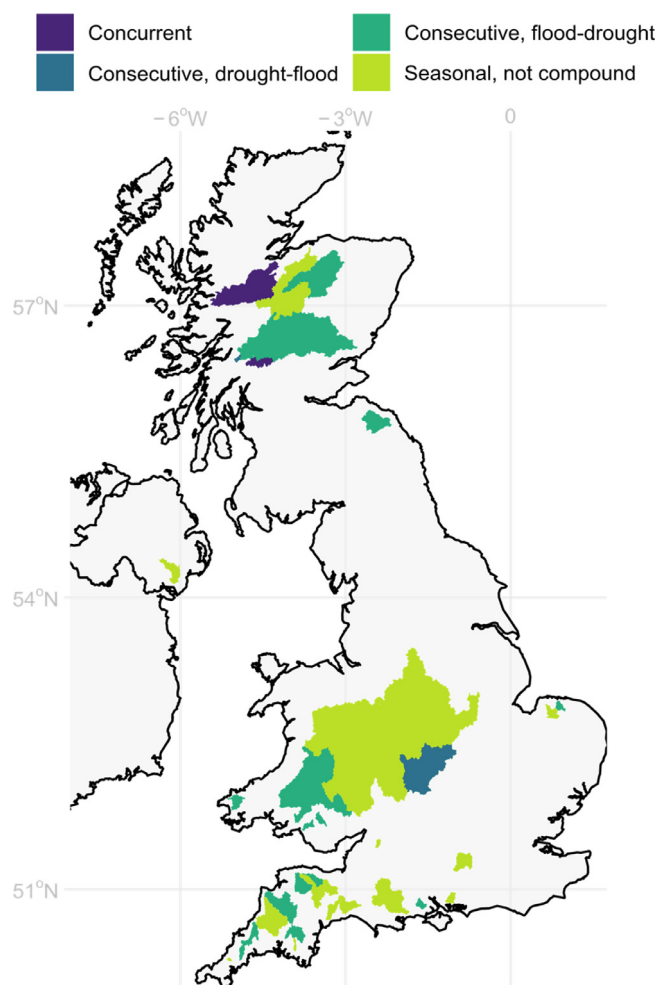
**Fig. 5.** Temporal clustering across the compound hydro-hazard hotspots.



**Fig. 6.** Mean change signal from the baseline to far-future, per mean annual metric, for each compound hydro-hazard hotspot. Note that colour scales are metric specific. For drought frequency, all hotspots see an increase of one event pa.

variances is equal to the total uncertainty, $T(t)$. The fraction of total variance $T(t)$ explained by each source of uncertainty $U(t)$, was determined as $U(t)/T(t)$ (3.3).

## 4. Results

### 4.1. Compound hydro-hazard hotspots

#### 4.1.1. Classification

Under RCP8.5, for the mean change signal (mean result from the multi-model ensemble), a total of 230 out of 239 catchments see an increase in the compound hydro-hazard in the far-future (2071–2099; Fig. 4a). Of these 230, more than half (144) lie within region II (Fig. 3), i.e. the concurrent increase in the mean annual flood metrics is in excess of the Table 2 flood thresholds; conversely, only 39 catchments lie within region III. Forty-seven compound hydro-hazard hotspots (region IV) were identified, accounting for 35% (47,785 km$^2$) of the total catchment area considered in this study.

The 47 compound hydro-hazard hotspots were further classified as per Table 1. Taking spatially clustered catchments first, the majority of these hotspots are concentrated in the south-west of England and Wales, as well as localised areas in the midlands and east of England (see Fig. 1 for regions). In Scotland, hotspots are located across East Scotland and the Highlands & Islands. Northern Ireland features a single hotspot in the east on the Upper Bann at Movallen. These hotspot regions may be described as being spatially compound at the inter-catchment level. Nine further catchments were identified as spatially compound
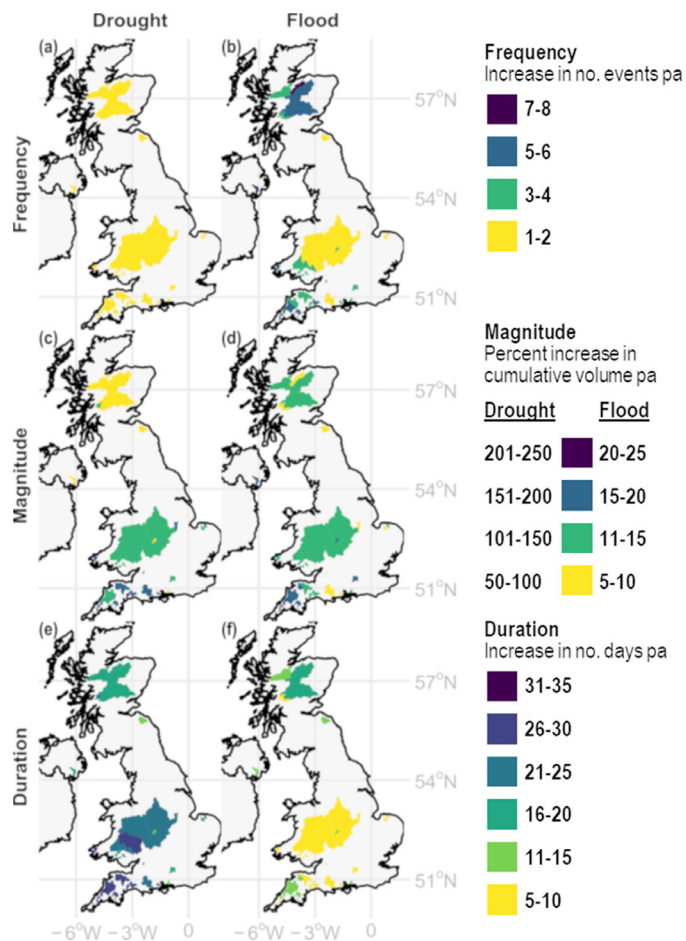
at the intra-catchment level, i.e. contain child catchments identified as hotspots (Fig. 4b–e). Across the UK, the hotspots are primarily headwater sub-catchments, or headwaters and the downstream outlet.

Fig. 5 further highlights two spatio-temporally compound hydro-hazard hotspot regions. The first is the North and East of Scotland region, containing six hotspots, including the Loch Ness and River Tay catchments, the largest lake and river by volume in the UK respectively. Drought is projected to occur in the summer months (JJA) for all hotspots in the region; the pressure in the region is further increased by the presence of the two concurrent hotspots. The second spatio-temporally compound hotspot region is located in the south-west, encompassing the south of Wales and South-west England. As shown in Fig. 4, a number of the catchments in this region are nested, with a number of headwaters identified as hotspots. In this region, there is a clustering of consecutive flood and drought events occurring over MAM and JJA respectively. With flood events preceding the drought, there may be an opportunity to store floodwaters and thereby offset the effect of drought in these regions.

#### 4.1.2. Change signal

Fig. 6 shows the projected mean change signal for the frequency, magnitude and duration metrics, for the 47 compound hydro-hazard hotspots identified. Beginning with drought frequency (Fig. 6a), a uniform increase of one event per annum is projected for all hotspots; this limited change is in part due to their longer temporal nature (relative to high flow events) and is therefore unsurprising (Collet et al., 2018).
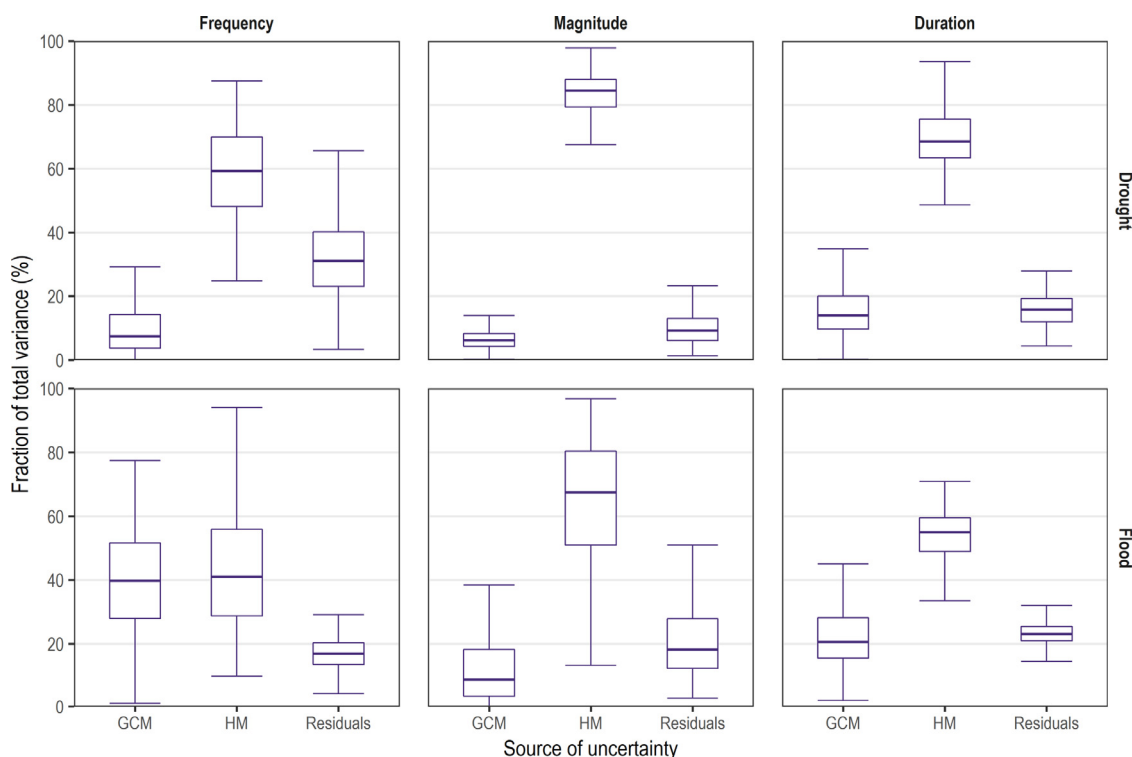
**Fig. 7.** Boxplots of the fraction of total variance explained by each source uncertainty, GCM, HM & residuals, across the 239 catchments (generalised trend).

With regards to flood frequency (Fig. 6b), the largest increases (up to +8 events per annum) are projected in Scotland (east and Highlands and Islands) and the south-west more generally (England and Wales).

The projected change in magnitude (Fig. 6c and d) reveals greater spatial variation across the compound hydro-hazard hotspots. In Scotland, floods are projected to increase by up to 14%, compared to a doubling for droughts (i.e. 110%). In the south-west of England, there is a similar picture for floods. By contrast, across east Wales and the west Midlands droughts generally see the greater increase in magnitude. For the drought mean change signal, a clear north-south divide is evident, with the flow deficit volume in the south at least double that of the north.

Fig. 6e and f reveals regional changes in event duration. In the south-west of the UK (Wales, the west Midlands and the south-west of England) the drought duration is projected to be 2–2.5 times greater than the rest of the UK. This trend is reversed for floods, with the largest increases projected across Scottish catchments (up to 20 days), by contrast, in the south, the increase in flood duration is, on average, 5–10 days.

In summary, the mean change signal suggests that the projected increase in drought magnitude is likely a product of the increase in duration rather than frequency (+1 event per annum). By comparison, flood events are projected to become more frequent, with smaller increases in the magnitude and duration of individual events. The spatial distribution and scale of the projections for magnitude and duration are consistent with Collet et al. (2018) (CMIP3, SRES A1B medium emissions scenario). The principle difference lies in the projected change in event frequency, with Collet et al. (2018) reporting parity in flood and drought frequency. The use of different emissions scenarios, HMs and GCMs may account for some of this lack of agreement. Despite these differences, it is appreciable to see the similarity in results.

### 4.2. Partitioned uncertainty

#### 4.2.1. All 239 catchments

The focus herein is on the uncertainty corresponding to the mean change signal projections and compound hydro-hazard hotspots, i.e. the

far-future (2071–2099). Fig. 7 shows the fraction of total variance associated with each source of uncertainty, for all 239 catchments, for the mean annual frequency, magnitude and duration metrics. By generalising across all catchments in this way, it can be seen that the HMs consistently represent the largest source of variability, whilst GCMs are the smallest. This finding is consistent with the validation, where GCMs were observed to converge for the majority of catchments. By metric, the (overall) greatest certainty can be seen to lie in the duration projections, as indicated by the limited range of values.

#### 4.2.2. Compound hydro-hazard hotspots

Figs. 8 and 9 (for drought and flood respectively) highlight spatial variability in the fraction of total variance across the compound hydro-hazard hotspots; it should also be noted that this is a UK specific finding and may not be the case in other parts of the world. In Scotland, the fraction of total variance associated with drought frequency is, relatively, evenly distributed across the three sources (Fig. 8a–c), whilst in the south the HMs represent the dominant source of uncertainty. The dominance of the HMs continues across the magnitude and duration (Fig. 8d–i), with limited localised variation. Van Lanen et al. (2013) show that groundwater representation and parameterisation was the dominant influence in HMs when reproducing drought characteristics. Consequently, the dominance of the HMs is most likely due to the fact that flows during drought conditions are typically dominated by groundwater, which is represented in different ways in the HMs.

In spite of the general trends observed in Fig. 7 previously, the GCMs represent the dominant source of uncertainty in flood frequency projections in Scotland (Fig. 9a). In the midlands and south of England this is more strongly dominated by the HM uncertainty (Fig. 9b), whilst in the south-west of England and south Wales the uncertainty is equally split across the sources. This may be attributed to the hydrogeological composition of the catchments; northern catchments tend to be faster-responding (low baseflow index, BFI; e.g. the Wensum at Fakenham), whilst catchments in the south tend to be dominated by groundwater (high BFI, e.g. the Dee at Polhollick). For flood magnitude (Fig. 9d–f),
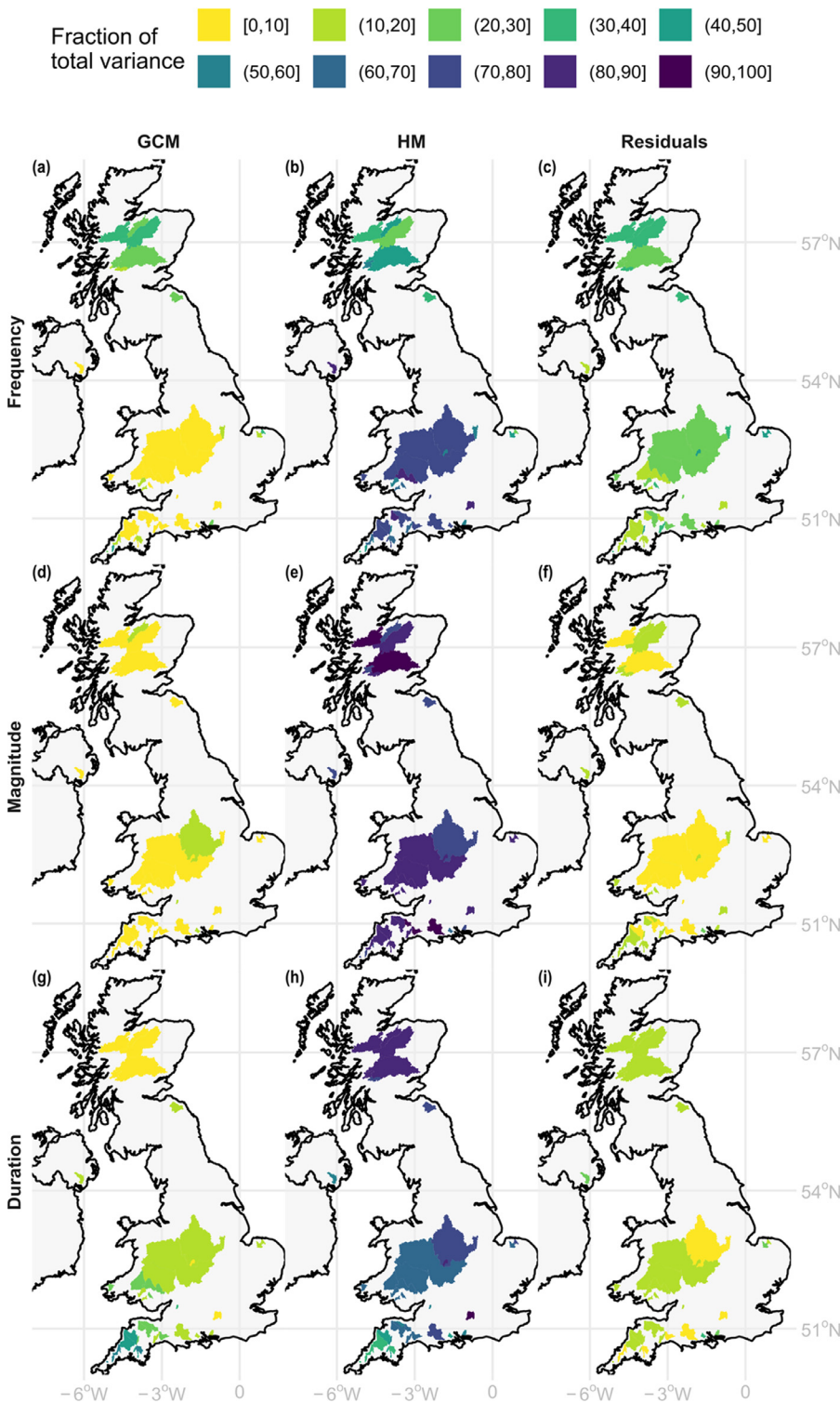
**Fig. 8.** Compound hydro-hazard hotspots, drought hazard. Fraction of total variance (%) explained by each source of modelling uncertainty: GCM, HM and residuals.

the GCMs have very little influence on the total variance across the UK; in the south-west and Wales the total variance is most strongly influenced by the structure of the HM (e.g. the model's ability to reproduce fast runoff processes). This is mirrored, albeit less strongly, in duration (Fig. 9g–i).

Broadly, Figs. 8 and 9 show agreement in the sources of uncertainty in the compound hydro-hazard hotspots and the catchments more generally. The additional understanding of the spatial variability of the total variance (uncertainty) and its components reveals a broad consistency

for droughts, with the exception of drought frequency, where differences in the north-south are in evidence. The sources of flood uncertainty are subject to greater localised variability, which may, in part, be due to topographical variation having a greater influence on results.

## 5. Discussion

In the context of future water insecurity, it is clear that consideration of the impact of compound hydro-hazards is essential. To build the
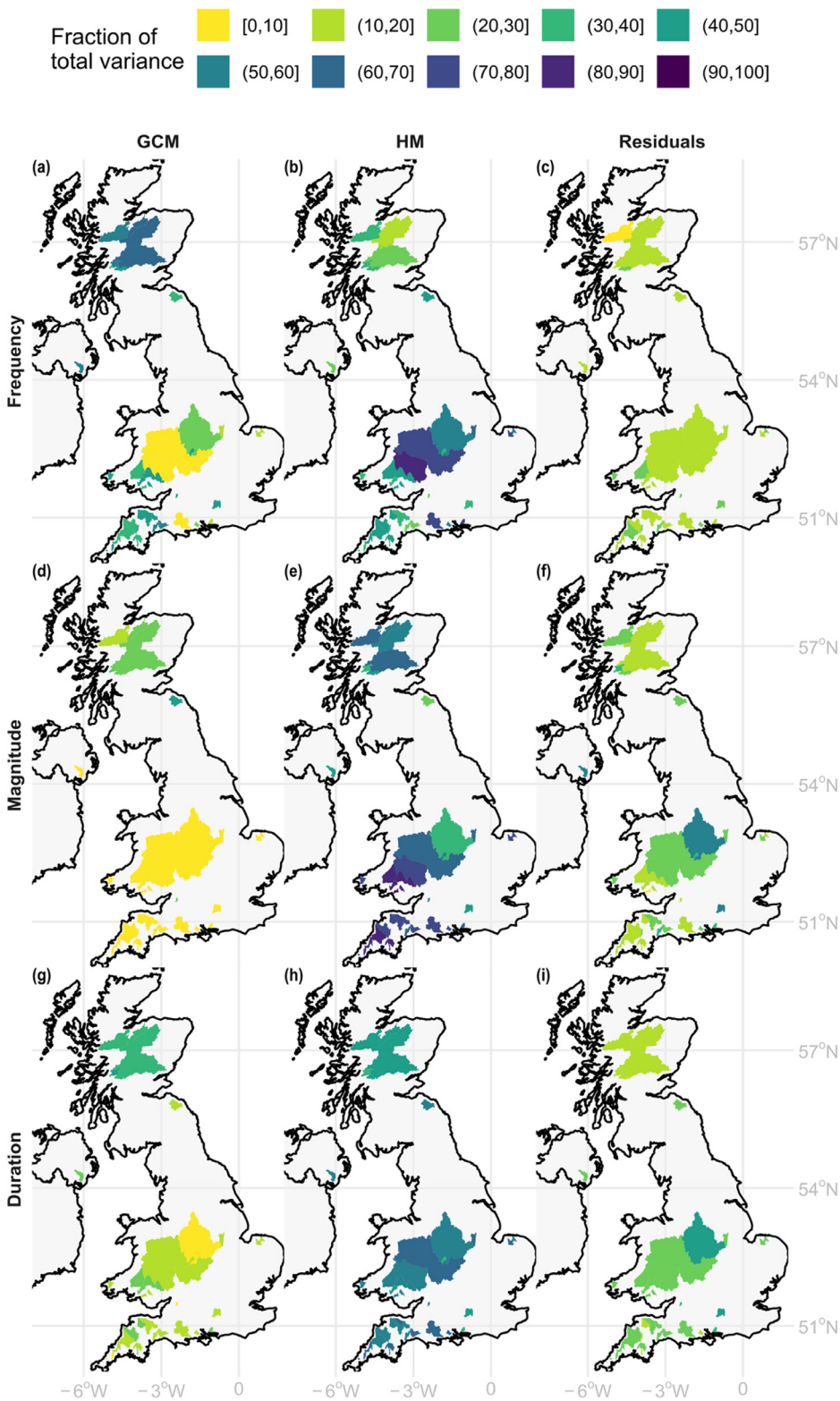
**Fig. 9.** Compound hydro-hazard hotspots, flood hazard. Fraction of total variance (%) explained by each source of modelling uncertainty, GCM, HM and residuals.

necessary resilience for climate change adaptation, there is a need to characterise the spatial and temporal clustering of compound extremes (Hao et al., 2018) and the associated uncertainty. To address this research gap, this study proposed a multi-stage (Fig. 2) impact and uncertainty framework for the identification of compound hydro-hazard hotspots.

In terms of the spatial distribution of the hazards, the results are consistent with multiple studies, thereby engendering greater confidence in the outputs. Marx et al. (2018) and Thober et al. (2018) saw similar regional trends for low and high flows respectively. Whilst these studies do use the same underlying data, these findings remain encouraging as the flow analyses are independent and employ different

methods. Additionally, as noted in the results, the location and scale of the mean change signals are also consistent with Collet et al. (2018), where the hydro-hazard hotspots arising from the SRES A1B emissions scenario across Great Britain were investigated.

### 5.1. Compound hydro-hazard hotspots

Satisfying objective one, the classification of compound hydro-hazard hotspots facilitates greater understanding of the spatial and temporal extent of concurrent changes in hydro-hazards. By focussing on the change per annum, the increase in intra-annual pressure was highlighted. To better understand the impact of the increase in hydro-hazard extremes, the identified compound hydro-hazard hotspots where further classified spatially and temporally. Whilst the impacts may propagate downstream, it is notable that in a number of cases, the hydro-hazard is less extreme in the lowest catchment. Half of the catchments were identified as temporally compound, with the majority projected as successive flood-drought events.

Consideration of the spatio-temporally compound hydro-hazard identified two hotspot regions, the north-east and south-west of the UK. In the north-east, approximately 10,000 m$^2$ is projected to be in drought in the summer months, with concurrent drought and flood in two catchments. Whilst Fig. 1 indicates that the population in these catchments is small, the large number of private water supplies in the region means the financial burden may still be high. Successive flood-droughts projected over MAM-JJA for a number of catchments in the south-west. With this improved understanding of the spatio-temporal nature of the hydro-hazards, it is possible to guide suitable adaptations, for example, storing flood waters for use during periods of drought. These findings clearly highlight the need for informed and tailored adaptation to improve overall resilience. Lastly, it is notable that the majority of the identified hotspots are projected to experience drought conditions in JJA, suggesting that a large proportion of the country may be subject to high levels of stress at the same time on an annual basis.

#### 5.1.1. Spatial distribution

When we explore the mean change signal associated with each metric, we can see that, under RCP8.5, confidence is greatest (least uncertainty) for changes in magnitude for both flood and drought (see Fig. 6). This change signal suggests that the UK should prepare for up to a 25% increase in high flow magnitude and a more extreme increase of 100–150% in the annual low flow deficit volume. Greater uncertainty surrounds the frequency and duration metrics. Differences in the mean change signal are clear across the UK, alongside variation in the source of this uncertainty. The high spatial discretisation across the UK makes these results particularly useful to modellers, consultants, water managers and planners; discussed in Section 5.3 Implications for water management.

#### 5.1.2. Characterisation of uncertainty

In this study, the dominant source of uncertainty associated with the hydroclimatological modelling arises from the HMs. The GCMs are, broadly, shown to converge, consistent with findings in Marx et al. (2018) and Thober et al. (2018) (across the UK). Knutti and Sedláček (2012) suggest that over the UK there is good robustness in model projections, thus a reasonably consistent change signal for the UK could indeed be expected. However, these findings are not replicated across Europe, where GCMs are shown to play a greater role in the uncertainty in the mean change signal (Marx et al., 2018; Thober et al., 2018). Similarly, studies in Australia suggest that the GCMs and RCMs contributed greater uncertainty than the HMs (Bennett et al., 2012). Consequently, it is important to understand the dominant controls upon uncertainty in climate modelling chains, and their roles locally.

As observed in this study, hydrological modelling may introduce substantial uncertainty (Vidal et al., 2016); their calibration to specific characteristics of the hydrological regime (e.g. high flows; Westerberg et al.,

2011; Pushpalatha et al., 2012) can play a significant role in this. Additional complexity is added when there is a lack of uniformity across the catchments considered, for example due to the hydrology (snowmelt, Marx et al., 2018; Thober et al., 2018; or groundwater, Collet et al., 2017 or geomorphology (karst, Hartmann, 2017).

An additional source of HM uncertainty is the portioning of precipitation into direct runoff and groundwater recharge. This is especially relevant in regions that have a strong groundwater influence (e.g. southeast UK) or where flow paths are short (disconnected from groundwater; e.g. urban areas).

### 5.2. Limitations

#### 5.2.1. EDgE dataset

The HMs within the EDgE project were calibrated to provide high model performance over the European domain using one parameter set per model. The specific catchments used in EDgE are not used to adjust the general pan-European parameter fields. It has been shown in earlier work that coherent parameter estimation on larger regions and catchments can help to reduce the difference in hydrological model parameterization (Samaniego et al., 2017), and thus could prove a valuable way forward to further reduce the hydrological uncertainty over Europe.

Additionally, the current version of the EDgE modelling chain does not include human water interactions. Reservoir operations, water withdrawals and irrigation all have an impact on the hydrological cycle and are likely to affect flow projections (particularly during periods of drought; Collet et al., 2015; Wanders and Wada, 2015). Although some of the models have the capacity to consider these processes, i.e. PCR-GLOBWB2, within EDgE increased consistency in the runoff routing (by using the mRM module) was deemed more important by the end-users.

Within EDgE, both the HMs have been deployed at a 5 km spatial resolution. For the GCMs specifically, this is below their native resolution of ~100 km, which affects their realism at smaller spatial scales. Downscaling with E-OBS data ensures that the statistical distribution of the meteorological variables within Europe is consistent with observations, most importantly accounting for the effect of hills and mountains that are not resolved at the native resolution of the GCMs. However, larger trends are consistent with the ~100 km resolution. In addition, due to computational demands, the large spatial extent of the EDgE domain necessitated the use of HMs which are known to perform well at coarser spatial resolutions. Consequently, at the local catchment scale, this might lead to a misrepresentation of the dominant hydrological processes in smaller UK catchments; a potential reason for the reduced performance of the HM PCR-GLOBWB2 specifically (see Appendix A.1).

#### 5.2.2. Metrics

Pronounced differences in the frequency of flood and drought events were observed. A number of catchments see all metrics exceed the hotspot threshold, with the exception of drought frequency. Consequently, catchments exhibiting severe relative changes, may not have been selected as hotspots. Following Collet et al. (2018), the inherent differences in flood and drought were accounted for using thresholds, defined to obtain a mean of three independent events per year on the baseline period (framework stage 1). Redundancy is present across the metrics of change, with magnitude and duration directly linked to frequency. Suggestive, perhaps, that the metrics may be better substituted for change per event per year, rather than simply per year.

#### 5.2.3. Uncertainty

An advantage of the QE-ANOVA framework is that it facilitates the disentangling of internal variability from the modelling uncertainty, thereby providing a more robust measure of the overall modelling uncertainty (Hingray and Saïd, 2014). However, in this study, it has not been possible to partition the uncertainty associated with internal variability into its component parts, this is due to (1) each modelling chain being run once and (2) the consideration of a single statistical downscaling

methodology. The effects of these component parts are however embedded within the residual uncertainty (Hingray and Saïd, 2014). The need for transient projections may be considered the main drawback of the QE-ANOVA framework.

*5.3. Implications for water management*

The results suggest that the future water security of the UK is dependent on the ability to adapt to projected changes in hydro-hazards. The first step towards adaptation is improving knowledge and understanding of regional changes, thereby allowing policy and decision makers to identify where in the UK compound hydro-hazards are most likely to intensify (i.e. hotspots). Consequently, a phased and focussed regional study can be directed towards such regions. Understanding of the dominant sources of uncertainty in projections (arising from the hydroclimatological modelling chain) means that these studies are able to utilise more focused, localised approaches that are aimed at constraining the dominant sources of uncertainty in the modelling chain. Examples include the application of sophisticated detailed modelling and the use of hydrodynamic models (Beevers et al., 2012; Balica et al., 2013), which may serve to constrain the uncertainty range of the new outputs (dependent on the physical characteristics of the catchments; e.g. Aitken et al., 2018). Further, a larger multi-model ensemble, capturing multiple evolutions of GCMs as well as multiple downscaling approaches, would allow to better quantify the sources of modelling uncertainty and internal variability. This would provide more detailed and valuable information to better deal with changes in the future and needed adaptation strategies in water management.

The intensification of the hydrologic dynamic (timing and seasonality of hydro-hazards) over a limited time frame represents a major challenge for future water management. In light of these observations, the incorporation of timing into the description of hydro-hazards is useful. For example, events not meeting the critical thresholds may still put a significant pressure on the system through concurrent action.

If we can improve our projections and quantify the associated uncertainty, we can then use this information in the adaptation process more explicitly. For example, understanding that we can be reasonably confident in the magnitude of change to high and low flows (as defined in this study and by Collet et al., 2018) allows for water managers to make better decisions in the design of adaptation measures.

## 6. Conclusions

Climate change is projected to amplify hydrological extremes at both ends of the spectrum, raising concerns and challenges for future water security. In response, there is a clear need to build resilience and improve adaptation for climate change. The first step towards achieving this requires knowledge and understanding of the degree of change in these extremes. At the outset of this paper, we argued that previous studies investigating this change have been inconsistent and limited in their focus. Collet et al. (2018) introduced a spatially coherent methodological framework for the projection of change in the compound hydro-hazards of flood and drought, however the ability to examine spatial and temporal trends was absent; additionally the sources of the uncertainty associated with the climate projections were not assessed which are particularly important for targeting future adaptation efforts. This paper sets out a novel, comprehensive approach to address both components.

For the UK, in the far-future (2071–2099), this study suggests an increase in compound hydro-hazard hotspots (mean change signal) across the country. Spatially compound hydro-hazards at the inter-catchment level are anticipated in the south-west of England and Wales and into the Midlands where there is a high population density. These areas are also indicated as spatially compound at the intra-catchment level, potentially further exacerbating impacts. This is also anticipated in the less densely populated north east of Scotland. Half of the identified hotspots are anticipated to be temporally concurrent or temporally successive within

the year, again exacerbating potential impacts on society. The northeast of Scotland and south-west of the UK were identified as spatio-temporally compound hotspot regions and are of particular concern.

The uncertainty in climate projections represents a key challenge in their practical application. In response, this study introduces a comprehensive impact and uncertainty methodological framework for the assessment of projected changes in hydro-hazards. The QE-ANOVA framework is used in this study, quantifying and partitioning the uncertainties associated with the flood and drought concurrently and across multiple metrics (frequency, magnitude and duration). This holistic depiction of uncertainty facilitates greater understanding of future water insecurity benefitting both researchers and water managers alike. The former, constantly seeking to quantify and understand uncertainty, are better informed as to where to focus their efforts, whilst the latter have access to information supporting more robust adaptation planning. The ability and advantages of the framework were highlighted through application across the UK using projections from the EDgE database. The hydrological models were identified as the largest source of variability in the projections of the mean change signal, in some instances exceeding 80% of total variance. This application raises important questions regarding the spatial variability of hydroclimatological modelling uncertainty.

In terms of water management planning, the findings allow for more focussed studies on significant areas of the country (with spatially and/or temporally compound hydro-hazard increases) with a view to improving the projections which inform the adaptation process. Reasonable confidence in the magnitude of the change in high and low flows across the UK at the end of the century might provide for immediate implementation.

## Contributions

LB is the PI of the *Water Resilient Cities: Climate uncertainty and urban vulnerability to hydro-hazards* project. Conceptualisation and design of methodology was undertaken by LB, LC and AV. The data was curated by the developers of the EDgE dataset: NW, ST, MP and RK and initial catchment selection was performed by LC and KS. Validation of the data was performed by AV. The formal analysis and investigation were principally undertaken by AV, with GF performing the extraction of the POT. The original draft was written by AV and LB, with contributions on catchment selection and the EDgE dataset provided by KS, NW, ST, MP and RK. All named authors contributed to the review and editing of the manuscript.

## Acknowledgements

## Supplementary materials

Supplementary material associated with this article can be found, in the online version, at doi:10.1016/j.advwatres.2019.05.019.

## Appendix A

*A.1. Validation*

The EDgE flow projections were validated against NRFA observed flow data on the baseline period (1971–2000) through graphical comparison of catchment cumulative distribution functions (CDF). Given the
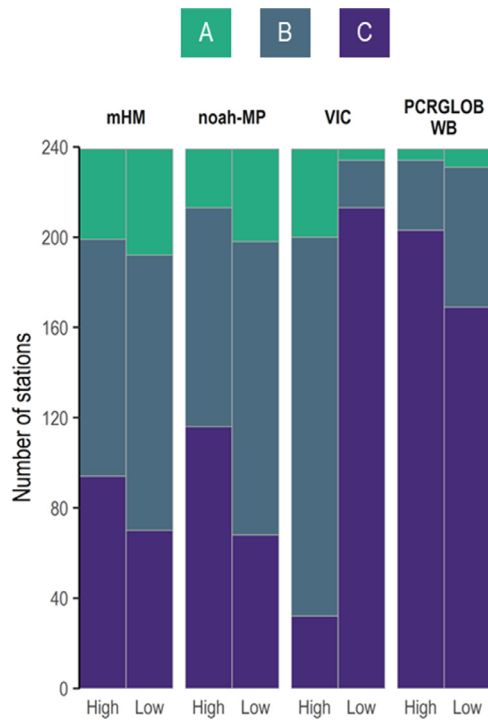
**Fig. A1.** By hydrological model, approximately 60% of catchments were graded B and above (see Table A1), with the exception of PCRGLOB-WB.

**Table A1**
Grades for the validation of the cumulative distribution functions.

| Grade | Shape | Scale |
|---|---|---|
| A | Good | Good; <25% error |
| B | Good | Acceptable; ~25% error |
| C | Poor | Poor; >25% error |

focus on hydro-hazards, the tails of the distribution (0–10th and 90–100th percentile) were graded (from A to C; Table A1) based on the replication of (1) the shape and (2) the flow magnitude of the CDF; variation in flow magnitude (scale) is expected due to the spread of uncertainty, though the ensemble mean should follow the observed CDF.

As observed in Marx et al. (2018), the validation revealed strong similarities across the five GCMs, with noticeable differences among the HMs. The HMs, with the exception of PCRGLOB-WB, showed a reasonable reproduction of the observed CDF with ~60% of catchments graded B and above (Table A1 and Fig. A1). However, flow projections output by PCRGLOB-WB2 were, often, uniform in nature, failing to capture high/low flow processes. Given the need to capture the range of uncertainty, this was not considered grounds for removal; however, the lack of clearly defined peak flows meant that extraction of events was not possible in the same manner as the other three HMs, consequently, flow projections from PCRGLOB-WB2 were removed.

### A.2. Catchment selection

In identifying catchments for inclusion, two lists were combined: Catchments included in the National Hydrological Monitoring Programme (NRFA, 2018), which are of significant interest for UK water re-
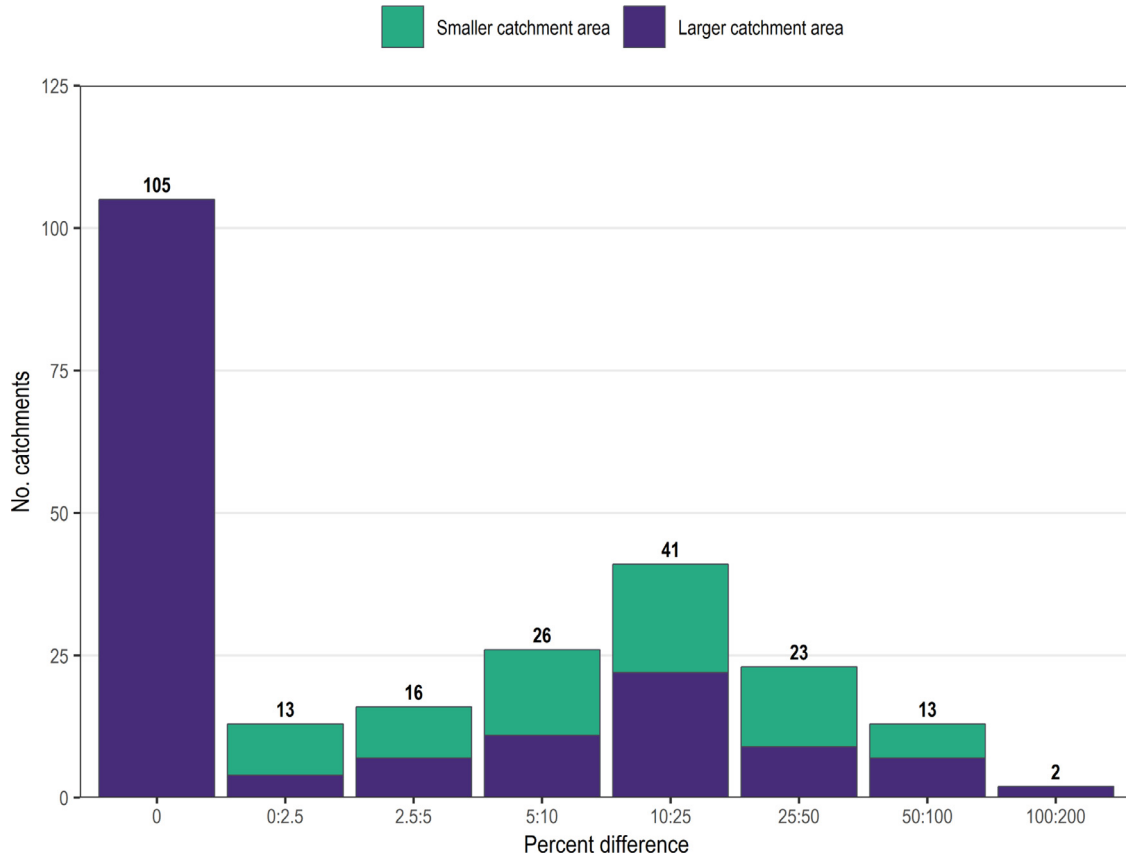


**Fig. A2.** Rounded to the nearest 25 km², all selected catchment areas demonstrated a percentage difference of less than 200%, with the majority (105 out of 239) exhibiting no difference. The limitations of the coarse spatial resolution of the EDgE projections are further considered in Section 5.2.

sources management; and the catchments from the Future Flows Hydrology dataset (Prudhomme et al., 2013), utilised by Collet et al. (2018) in the development of the hydro-hazard hotspot methodology.

The data requirements for the validation and quantification of uncertainty led to the rejection of catchments with less than 15 years of observed flow data on the baseline period (1971–2000), reducing the number of catchments from 254 to 239. The distribution of the selected catchments is detailed in Fig. 1.

Due to the pan-European domain of EDgE, projections are produced at a 5 km spatial resolution (25 km$^2$ grid cell); consequently, catchments with an upstream area of less than 25 km$^2$ were excluded in this study. Given the coarse resolution, it was necessary to manually correct to the nearest EDgE grid-cell on the river network, with an upstream contributing area as close to the NRFA catchment area as possible. Rounded to the nearest 25 km$^2$, all selected catchment areas demonstrated a percentage difference of less than 200%, with 105 out of 239 exhibiting no difference (Fig. A2).
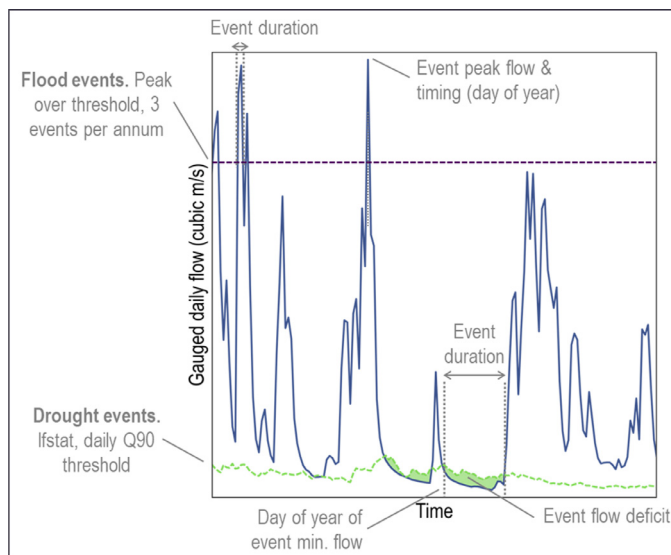
### A.3. Event extraction



**Fig. A3.** Example flow time-series with the flood and drought thresholds marked. Examples of each event metric are indicated.
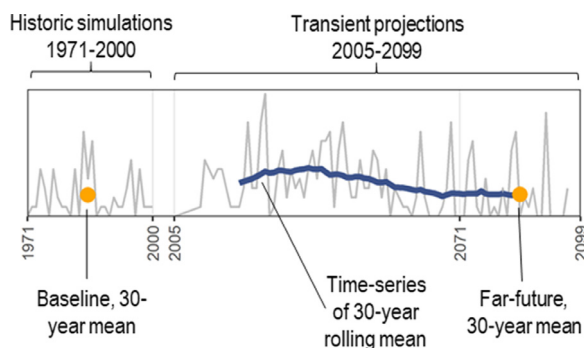


**Fig. A4.** Time-series for an exemplar annual summary metric. The time periods representing the historic simulations and transient projections are indicated. The overlain blue line represents the 30-year rolling mean over 2005–2099, whilst the orange points represent the 30-year mean at two particular points in time. A 30-year rolling mean over the entire time-series is not possible due to a 5-year break between the historic simulations and projections.

**Table A2**
Equations for the determination of the annual summary metrics.

|            | Drought                      | Flood                          |
|------------|------------------------------|--------------------------------|
| *Frequency* | Σ Events                    |                                |
| *Duration*  | Σ Event duration            |                                |
| *Magnitude* | Σ Flow deficit              | Max. peak flow                 |
| *Timing*    | Day of year of min. flow    | Day of year of max. peak flow  |

### References

Aitken, G., Beevers, L., Collet, L., Maravat, C., 2018. Future flood extents: capturing the uncertainty associated with climate change. International Environmental Modelling and Software Society. Fort Collins, USA 26-28th June.

Balica, S.F., Popescu, I., Beevers, L., Wright, N.G., 2013. Parametric and physically based modelling techniques for flood risk and vulnerability assessment: a comparison. Environ. Model. Softw. 41:, 84–92. https://doi.org/10.1016/j.envsoft.2012.11.002.

Bayliss, A.C., Jones, R.C., 1993. Peaks-Over-Threshold Flood Database: Summary Statistics and Seasonality. Wallingford. Institute of Hydrology, Oxfordshire.

Beevers, L., Douven, W., Lazuardi, H., Verheij, H., 2012. Cumulative impacts of road developments in floodplains. Transp. Res. Part D 17 (5), 398–404. https://doi.org/10.1016/j.trd.2012.02.005.

Bennett, J.C., Ling, F.L.N., Post, D.A., Grose, M.R., Corney, S.P., Graham, B., Holz, G.K., Katzfey, J.J., Bindoff, N.L., 2012. High-resolution projections of surface water availability for Tasmania. Hydrol. Earth Syst. Sci. 16 (5), 1287–1303. http://dx.doi.org/10.5194/hess-16-1287-2012.

Butterworth, K., Margolis, Z., 2019. From Drought to Flooding Rains as Farmers Celebrate Drenching in Queensland's West. ABC News, Australia Available: https://www.abc.net.au/news/rural/2019-02-04/from-drought-to-flooding-rains-in-western-queensland/10776576.

C3S, 2018. EDgE CoPernicus Climate Change Service. Copernicus Available: http://edge.climate.copernicus.eu .

Cherkauer, K.A., Bowling, L.C., Lettenmaier, D.P., 2003. Variable infiltration capacity cold land process model updates. Global Planet. Change 38 (1), 151–159. https://doi.org/10.1016/S0921-8181(03)00025-0.

Christierson, B.v., Vidal, J.-P., Wade, S.D., 2012. Using UKCP09 probabilistic climate information for UK water resource planning. J. Hydrol. 424–425, 48–67. http://dx.doi.org/10.1016/j.jhydrol.2011.12.020.

Collet, L., Beevers, L., Prudhomme, C., 2017. Assessing the impact of climate change and extreme value uncertainty to extreme flows across Great Britain. Water 9 (2), 103. https://doi.org/10.3390/w9020103.

Collet, L., Harrigan, S., Prudhomme, C., Formetta, G., Beevers, L., 2018. Future hot-spots for hydro-hazards in Great Britain: a probabilistic assessment. Hydrol. Earth Syst. Sci. 22 (10), 5387–5401. https://doi.org/10.5194/hess-22-5387-2018.

Collet, L., Ruelland, D., Estupina, V.B., Dezetter, A., Servat, E., 2015. Water supply sustainability and adaptation strategies under anthropogenic and climatic changes of a meso-scale Mediterranean catchment. Sci. Total Environ. 536:, 589–602. https://doi.org/10.1016/j.scitotenv.2015.07.093.

CSIRO, 2018. State of the climate 2018. ISBN: 978-1-925315-97-4. Commonwealth Scientific and Industrial Research Organisation, Australia.

Daniel Koffler, Tobias Gauster & Laaha, G. 2016. lfstat: cCalculation of low flow statistics for daily stream flow data. R package version 0.9.4. https://CRAN.R-project.org/package=lfstat.

Dankers, R., Arnell, N.W., Clark, D.B., Falloon, P.D., Fekete, B.M., Gosling, S.N., Heinke, J., Kim, H., Masaki, Y., Satoh, Y., Stacke, T., Wada, Y., Wisser, D., 2014. First look at changes in flood hazard in the Inter-Sectoral Impact Model Intercomparison Project ensemble. Proc. Natl. Acad. Sci. 111 (9), 3257–3261. https://doi.org/10.1073/pnas.1302078110.

Devkota, L.P., Gyawali, D.R., 2015. Impacts of climate change on hydrological regime and water resources management of the Koshi River Basin, Nepal. J. Hydrol. 4:, 502–515. https://doi.org/10.1016/j.ejrh.2015.06.023.

Donnelly, C., Greuell, W., Andersson, J., Gerten, D., Pisacane, G., Roudier, P., Ludwig, F., 2017. Impacts of climate change on European hydrology at 1.5, 2 and 3 degrees mean global warming above preindustrial level. Clim. Change 143 (1), 13–26. https://doi.org/10.1007/s10584-017-1971-7.

Fischer, E.M., Knutti, R., 2016. Observed heavy precipitation increase confirms theory and early models. Nat. Clim. Change 6 (, 11 ), 986. https://doi.org/10.1038/nclimate3110.

Formetta, G., Bell, V., Stewart, E., 2018. Use of flood seasonality in pooling-group formation and quantile estimation: an application in Great Britain. Water Resour. Res. 54 (2), 1127–1145. https://doi.org/10.1002/2017WR021623.

Gosling, S.N., Zaherpour, J., Mount, N.J., Hattermann, F.F., Dankers, R., Arheimer, B., Breuer, L., Ding, J., Haddeland, I., Kumar, R., Kundu, D., Liu, J., van Griensven, A., Veldkamp, T.I.E., Vetter, T., Wang, X., Zhang, X., 2017. A comparison of changes in river runoff from multiple global and catchment-scale hydrological models under global warming scenarios of 1°C, 2°C and 3°C. Clim. Change 141 (3), 577–595. https://doi.org/10.1007/s10584-016-1773-3.

Guha-Sapir, D., Below, R., Hoyois, P., 2018. EM-DAT the Emergency Events Database Available: https://www.emdat.be/ .

Gustard, A., Demuth, S., 2009. Manual on Low-flow Estimation and Prediction. Publications Board World Meteorological Organization (WMO), Geneva, Switzerland Operational Hydrology Report No. 50.

Hao, Z., Singh, V.P., Hao, F., 2018. Compound extremes in hydroclimatology: a review. Water 10 (6), 718.

Hartmann, A., 2017. Experiences in calibrating and evaluating lumped karst hydrological models. *Geol. Soc. Lond. Spec. Publ.* 466. http://dx.doi.org/10.1144/sp466.18.

Hawkins, E., Sutton, R., 2009. The potential to narrow uncertainty in regional climate predictions. *Bull. Am. Meteorol. Soc.* 90 (8), 1095–1108. http://dx.doi.org/10.1175/2009bams2607.1.

Hingray, B., Blanchet, J., Evin, G., Vidal, J.-P., 2019. Uncertainty component estimates in transient climate projections. *Clim. Dyn.* doi:10.1007/s00382-019-04635-1.

Hingray, B., Saïd, M., 2014. Partitioning internal variability and model uncertainty components in a multimember multimodel ensemble of climate projections. *J. Clim.* 27 (17), 6779–6798. https://doi.org/10.1175/jcli-d-13-00629.1.

Institute of Hydrology, 1999. Flood Estimation Handbook. Volume 3: Statistical Procedures for Flood Frequency Estimation. Centre for Ecology & Hydrology, Wallingford, Oxfordshire.

IPCC, 2012. Managing the risks of extreme events and disasters to advance climate change adaptation. In: FIELD, C.B., BARROS, V., STOCKER, T.F., QIN, D., DOKKEN, D.J., EBI, K.L., et al. (Eds.), A Special Report of Working Groups I and II of the Intergovernmental Panel on Climate Change. Cambridge University Press, Cambridge, UK, and New York, NY, USA.

Kay, A.L., Crooks, S.M., Davies, H.N., Prudhomme, C., Reynard, N.S., 2014a. Probabilistic impacts of climate change on flood frequency using response surfaces I: England and Wales. *Reg. Environ. Change* 14 (3), 1215–1227. http://dx.doi.org/10.1007/s10113-013-0563-y.

Kay, A.L., Crooks, S.M., Davies, H.N., Reynard, N.S., 2014b. Probabilistic impacts of climate change on flood frequency using response surfaces II: scotland. *Reg. Environ. Change* 14 (3), 1243–1255. http://dx.doi.org/10.1007/s10113-013-0564-x.

Knutti, R., Sedláček, J., 2012. Robustness and uncertainties in the new CMIP5 climate model projections. *Nat. Clim. Change* 3 (4), 369. http://dx.doi.org/10.1038/nclimate1716.

Kumar, R., Livneh, B., Samaniego, L., 2013. Toward computationally efficient large-scale hydrologic predictions with a multiscale regionalization scheme. *Water Resour. Res.* 49 (9), 5700–5714. https://doi.org/10.1002/wrcr.20431.

Li, Q., Yang, T., Qi, Z., Li, L., 2018. Spatiotemporal Variation of snowfall to precipitation ratio and its implication on water resources by a regional climate model over Xinjiang, China. Water 10 (10), 1463. https://doi.org/10.3390/w10101463.

Liang, X., Wood, E.F., Lettenmaier, D.P., 1996. Surface soil moisture parameterization of the VIC-2 L model: evaluation and modification. *Global Planet. Change* 13 (1), 195–206. https://doi.org/10.1016/0921-8181(95)00046-1.

Manfreda, S., Caylor, K., 2013. On the vulnerability of water limited ecosystems to climate change. Water 5 (2), 819. https://doi.org/10.3390/w5020819.

Marx, A., Kumar, R., Thober, S., Rakovec, O., Wanders, N., Zink, M., Wood, E.F., Pan, M., Sheffield, J., Samaniego, L., 2018. Climate change alters low flows in Europe under global warming of 1.5, 2, and 3 °C. Hydrol. Earth Syst. Sci. 22 (2), 1017–1032. https://doi.org/10.5194/hess-22-1017-2018.

McSweeney, C.F., Jones, R.G., 2016. How representative is the spread of climate projections from the 5 CMIP5 GCMs used in ISI-MIP. *Clim. Serv.* 1, 24–29. https://doi.org/10.1016/j.cliser.2016.02.001.

National Research Council, 1999. Hydrologic Hazards Science at the U.S. Geological Survey. Washington, DC, The National Academies Press.

Niu, G.-Y., Yang, Z.-L., Mitchell, K.E., Chen, F., Ek, M.B., Barlage, M., Kumar, A., Manning, K., Niyogi, D., Rosero, E., Tewari, M., Xia, Y., 2011. The community Noah land surface model with multiparameterization options (Noah-MP): 1. Model description and evaluation with local-scale measurements. *J. Geophys. Res.* 116 (D12) https://doi.org/10.1029/2010JD015139.

NRFA, 2018. National Hydrological Monitoring Programme. National River Flow Archive, Centre for Ecology and Hydrology, Wallingford Available: https://nrfa.ceh.ac.uk/nhmp .

ONS, 2018. Overview of the UK Population. Office for National Statistics, Newport, United Kingdom November 2018.

Parry, S., Marsh, T., Kendon, M., 2013. 2012: from drought to floods in England and Wales. Weather 68 (10), 268–274. https://doi.org/10.1002/wea.2152.

Prudhomme, C., Haxton, T., Crooks, S., Jackson, C., Barkwith, A., Williamson, J., Kelvin, J., Mackay, J., Wang, L., Young, A., Watts, G., 2013. Future flows hydrology: an ensemble of daily river flow and monthly groundwater levels for use for climate change impact assessment across Great Britain. Earth Syst. Sci. Data 5 (1), 101–107. https://doi.org/10.5194/essd-5-101-2013.

Prudhomme, C., Young, A., Watts, G., Haxton, T., Crooks, S., Williamson, J., Davies, H., Dadson, S., Allen, S., 2012. The drying up of Britain? A national estimate of changes in seasonal river flows from 11 regional climate model simulations. *Hydrol. Process.* 26 (7), 1115–1118. http://dx.doi.org/10.1002/hyp.8434.

Pushpalatha, R., Perrin, C., Moine, N.L., Andréassian, V., 2012. A review of efficiency criteria suitable for evaluating low-flow simulations. *J. Hydrol.* 420-421, 171–182. https://doi.org/10.1016/j.jhydrol.2011.11.055.

Reis, S., Liska, T., Steinle, S., Carnell, E., Leaver, D., Roberts, E., Vieno, M., Beck, R., Dragosits, U., 2017. UK gridded population 2011 based on Census 2011 and Land Cover Map 2015. NERC Environ. Inf. Data Centre. https://doi.org/10.5285/0995e94d-6d42-40c1-8ed4-5090d82471e1.

Riahi, K., Rao, S., Krey, V., Cho, C., Chirkov, V., Fischer, G., Kindermann, G., Nakicenovic, N., Rafaj, P., 2011. RCP 8.5—a scenario of comparatively high greenhouse gas emissions. *Clim. Change* 109 (1), 33. http://dx.doi.org/10.1007/s10584-011-0149-y.

Samaniego, L., Kumar, R., Attinger, S., 2010. Multiscale parameter regionalization of a grid-based hydrologic model at the mesoscale. *Water Resour. Res.* 46 (5). https://doi.org/10.1029/2008WR007327.

Samaniego, L., Kumar, R., Thober, S., Rakovec, O., Zink, M., Wanders, N., Eisner, S., Müller Schmied, H., Sutanudjaja, E.H., Warrach-Sagi, K., Attinger, S., 2017. Toward seamless hydrologic predictions across spatial scales. Hydrol. Earth Syst. Sci. 21 (9), 4323–4346. http://dx.doi.org/10.5194/hess-21-4323-2017.

Samaniego, L., Thober, S., Kumar, R., Wanders, N., Rakovec, O., Pan, M., Zink, M., Sheffield, J., Wood, E.F., Marx, A., 2018. Anthropogenic warming exacerbates European soil moisture droughts. *Nat. Clim. Change* 8 (5), 421–426. https://doi.org/10.1038/s41558-018-0138-5.

Sayers, P., Horritt, M., Penning-Rowsell, E., McKenzie, A., Thompson, D., 2016. The analysis of future flood risk in the UK using the Future Flood Explorer. *E3S Web Conf.* 7, 21005.

Schleussner, C.-F., Pfleiderer, P., Fischer, E.M., 2017. In the observational record half a degree matters. *Nat. Clim. Change* 7:, 460. https://doi.org/10.1038/nclimate3320.

Smith, K.A., Wilby, R.L., Broderick, C., Prudhomme, C., Matthews, T., Harrigan, S., Murphy, C., 2018. Navigating cascades of uncertainty — as easy as ABC? Not quite…. *J. Extreme Events* 05 (01), 1850007. http://dx.doi.org/10.1142/s2345737618500070.

Sutanudjaja, E.H., van Beek, R., Wanders, N., Wada, Y., Bosmans, J.H.C., Drost, N., van der Ent, R.J., de Graaf, I.E.M., Hoch, J.M., de Jong, K., Karssenberg, D., López López, P., Peßenteiner, S., Schmitz, O., Straatsma, M.W., Vannametee, E., Wisser, D., Bierkens, M.F.P., 2018. PCR-GLOBWB 2: a 5 arcmin global hydrological and water resources model. Geosci. Model Dev. 11 (6), 2429–2453. https://doi.org/10.5194/gmd-11-2429-2018.

Taylor, K.E., Stouffer, R.J., Meehl, G.A., 2011. A Summary of the CMIP5 Experiment Design. Program for Climate Model Diagnosis and Intercomparison, Lawrence Livermore National Laboratory, California, United States.

Thober, S., Cuntz, M., Kelbling, M., Kumar, R., Mai, J., Samaniego, L., 2019. The multiscale routing model mRM v1.0: simple river routing at resolutions from 1 to 50 km. Geosci. Model Dev. Discuss. 2019, 1–26. https://doi.org/10.5194/gmd-2019-13.

Thober, S., Kumar, R., Wanders, N., Marx, A., Pan, M., Rakovec, O., Samaniego, L., Sheffield, J., Wood, E.F., Zink, M., 2018. Multi-model ensemble projections of European river floods and high flows at 1.5, 2, and 3 degrees global warming. *Environ. Res. Lett.* 13 (1), 014003.

Van Lanen, H.A.J., Wanders, N., Tallaksen, L.M., Van Loon, A.F., 2013. Hydrological drought across the world: impact of climate and physical catchment structure. Hydrol. Earth Syst. Sci. 17 (5), 1715–1732. http://dx.doi.org/10.5194/hess-17-1715-2013.

Vidal, J.P., Hingray, B., Magand, C., Sauquet, E., Ducharne, A., 2016. Hierarchy of climate and hydrological uncertainties in transient low-flow projections. Hydrol. Earth Syst. Sci. 20 (9), 3651–3672. https://doi.org/10.5194/hess-20-3651-2016.

Vousdoukas, M.I., Mentaschi, L., Voukouvalas, E., Verlaan, M., Jevrejeva, S., Jackson, L.P., Feyen, L., 2018. Global probabilistic projections of extreme sea levels show intensification of coastal flood hazard. *Nat. Commun.* 9 (1), 2360. http://dx.doi.org/10.1038/s41467-018-04692-w.

Wanders, N., Thober, S., Kumar, R., Pan, M., Sheffield, J., Samaniego, L., Wood, E.F., 2018. Development and evaluation of a pan-european multimodel seasonal hydrological forecasting system. *J. Hydrometeorol.* 20 (1), 99–115. https://doi.org/10.1175/JHM-D-18-0040.1.

Wanders, N., Wada, Y., 2015. Decadal predictability of river discharge with climate oscillations over the 20th and early 21st century. *Geophys. Res. Lett.* 42 (24), 689. 1010, 695 https://doi.org/10.1002/2015GL066929 .

Warmink, J.J., Janssen, J.A.E.B., Booij, M.J., Krol, M.S., 2010. Identification and classification of uncertainties in the application of environmental models. *Environ. Model. Softw.* 25 (12), 1518–1527. http://dx.doi.org/10.1016/j.envsoft.2010.04.011.

Warszawski, L., Frieler, K., Huber, V., Piontek, F., Serdeczny, O., Schewe, J., 2014. The Inter-Sectoral Impact Model Intercomparison Project (ISI–MIP): project framework. *Proc. Natl. Acad. Sci.* 111 (9), 3228–3232. https://doi.org/10.1073/pnas.1312330110.

Watts, G., Battarbee, R.W., Kernan, M., Bloomfield, J.P., Jackson, C.R., Mackay, J., Crossman, J., Whitehead, P.G., Daccache, A., Hess, T., Knox, J., Weatherhead, K., Durance, I., Ormerod, S.J., Elliott, J.A., Hannaford, J., Kay, A.L., Monteith, D.T., Garner, G., Hannah, D.M., Rance, J., Stuart, M.E., Wade, A.J., Wade, S.D., Wilby, R.L., 2015. Climate change and water in the UK – past changes and future prospects. *Prog. Phys. Geogr.* 39 (1), 6–28. http://dx.doi.org/10.1177/0309133314542957.

Westerberg, I.K., Guerrero, J.L., Younger, P.M., Beven, K.J., Seibert, J., Halldin, S., Freer, J.E., Xu, C.Y., 2011. Calibration of hydrological models using flow-duration curves. Hydrol. Earth Syst. Sci. 15 (7), 2205–2227. https://doi.org/10.5194/hess-15-2205-2011.

Yang, Z.-L., Niu, G.-Y., Mitchell, K.E., Chen, F., Ek, M.B., Barlage, M., Longuevergne, L., Manning, K., Niyogi, D., Tewari, M., Xia, Y., 2011. The community Noah land surface model with multiparameterization options (Noah-MP): 2. Evaluation over global river basins. *J. Geophys. Res.* 116 (D12) https://doi.org/10.1029/2010JD015140.